Colloids and Surfaces A: Physicochemical and Engineering Aspects 713 (2025) 136534

Contents lists available at ScienceDirect

Colloids and Surfaces A: Physicochemical and Engineering Aspects

journal homepage: www.elsevier.com/locate/colsurfa

Partially hydrolyzed poly(2-oxazoline)s as a new class of biocompatible modifiers of montmorillonites for the adsorption and decontamination of the organophosphate paraoxon

Zuzana Kroneková [a,1], Luboš Jankovič [b,2], Zuzana Mošková [a], Alžbeta Minarčíková [a], Hanna Zhukouskaya [c,3], Jan Kučka [c,4], Miroslav Vetrík [c,5], Martin Hrubý [c,6], Juraj Kronek [a,*,7]

[a] Department for Biomaterials Research, Polymer Institute, Slovak Academy of Sciences, Dúbravská cesta 9, Bratislava 845 41, Slovakia
[b] Institute of Inorganic Chemistry, Slovak Academy of Sciences, Dúbravská cesta 9, Bratislava 845 41, Slovakia
[c] Institute of Macromolecular Chemistry, Czech Academy of Sciences, Heyrovského náměstí 2, Prague 162 066, Czech Republic

HIGHLIGHTS

- Poly(2-ethyl-2-oxazoline-co-ethylene imine)s are for the first time used for the organo-modification of montmorillonites.
- Composition of copolymers and amount of copolymer loaded has high impact on basal spacing values.
- Organo-modification of montmorillonites with prepared copolymers decreases *in vitro* cytotoxic effects observed for montmorillonites.
- Organo-modified montmorillonites accelerate hydrolytic decomposition of paraoxon as a representative of organophosphate.

GRAPHICAL ABSTRACT

Partially hydrolyzed poly(2-oxazoline)s as new class of biocompatible modifiers of montmorillonites for sorption and decontamination of organic molecules
Statistical copolymers of 2-ethyl-2-oxazoline and ethylene imine of different molar fractions prepared by partial acidic hydrolysis of poly(2-ethyl-2-oxazoline) represent an effective tool for organo-modification of layered silicates. Modified montmorillonites decrease *in vitro* cytotoxic effects of montmorillonites and accelerate hydrolytic decomposition of paraoxon as a representative of organophosphate pesticide and warfare agents compared to pristine montmorillonite.

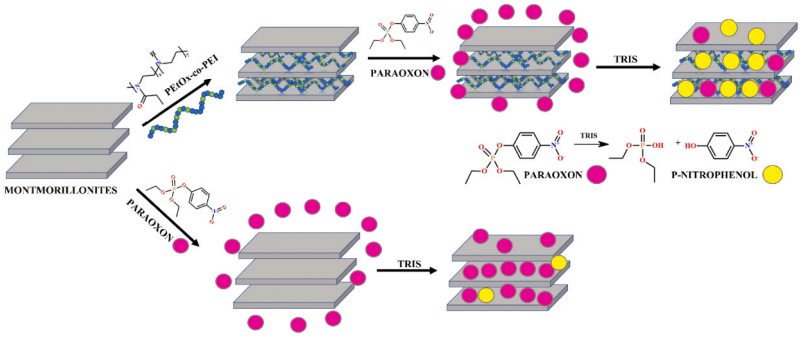

* Corresponding author.
E-mail address: juraj.kronek@savba.sk (J. Kronek).
[1] 0000–0002-0265–8901
[2] 0000–0002-2875–6278
[3] 0009–0004-4691–8869
[4] 0000–0003-2489–5315
[5] 0000–0002-0118–3799
[6] 0000–0002-5075–261X
[7] 0000–0002-0348–9740

https://doi.org/10.1016/j.colsurfa.2025.136534
Received 15 November 2023; Received in revised form 19 February 2025; Accepted 25 February 2025
Available online 26 February 2025

ARTICLE INFO

Keywords:
Poly(2-oxazoline)
Poly(ethylene imine)
Cationic polymers
Montmorillonite
Clay minerals
Partial hydrolysis
Biocompatibility
Adsorption
Paraoxon

ABSTRACT

Cationic (co)polymers play an important role in many (bio)applications, such as drug and gene delivery, antimicrobial agents, integral parts of hydrogels, and others. Here, we present cationic copolymers prepared by partial hydrolysis of poly(2-ethyl-2-oxazoline) as a new type of polymeric modifier of clay minerals with improved biocompatibility toward potential utilization in biomedical and environmental applications. Statistical poly(2-ethyl-2-oxazoline-co-ethylene imine)s (PEtOx-co-PEI) of different compositions (degree of hydrolysis 9, 12, 22, 28, 55 and 56 %, respectively) are prepared by a two-step synthetic protocol consisting of a living cationic ring-opening polymerization of 2-ethyl-2-oxazoline and the subsequent acidic hydrolysis of poly(2-ethyl-2-oxazoline). We demonstrate that above 22 mol% of ethylene imine (EI) units, prepared copolymers are positively charged as seen from the zeta potential measurements. The XRD patterns of the powder samples of PEtOx-co-PEI modified organoclays are analyzed in order to evaluate the impact of the initial concentration of copolymers, used for sample preparation, on the changes in basal spacing value (d_{001}), reflecting the expansion of the interlayer space. We observe the expansion of the interlayer space in montmorillonite (MMT), a clay mineral from the smectite group, dependently on the composition of copolymers and the content of the copolymer in MMT. The presence of copolymers in the interlayer space of MMT decreases *in vitro* cytotoxicity of virgin MMT as determined in 3T3 mice fibroblasts. MMT modified with PEtOx-co-PEI can have strong potential as a drug delivery vehicle, for tissue engineering applications, or as a sorption material. However, a key application explored in this study is the removal and degradation of the organophosphate paraoxon, a highly toxic insecticide and potent chemical warfare agent. Here, we show adsorption and, importantly, also hydrolytic decomposition of the model substrate paraoxon as a representative of organophosphates at physiological neutral pH (Tris buffer pH 7.4). Hydrolysis of paraoxon is easy to follow due to chromogenicity, where the spectral change is given by the release of 4-nitrophenolate with a different UV–VIS spectrum than paraoxon. MMT modified with the soluble partially hydrolyzed poly(2-ethyl-2-oxazoline) with 59 mol% EI units significantly increases the hydrolysis rate of paraoxon compared to non-modified pristine MMT. These findings highlight the potential of PEtOx-co-PEI-modified MMT for biomedical applications and environmental remediation, particularly in detoxifying hazardous organophosphates.

1. Introduction

Layered clay minerals play an important role in the design of advanced materials in many (bio)applications, e.g., as sorption materials and flocculants, catalysts, fillers for (nano)composites, drug delivery systems, or materials for tissue engineering [1–3]. Montmorillonite (MMT), a member of the smectite group of minerals, is renowned for its unique structural and physicochemical properties, making it a versatile material in various scientific and industrial applications. It is characterized by a layered structure consisting of two tetrahedral sheets sandwiching an octahedral sheet. This 2:1 structure results in a high cation exchange capacity (CEC), significant surface area, and the ability to swell upon hydration. The structure of MMT allows for the incorporation and exchange of various cations, such as Na^+, Ca^{2+}, and Mg^{2+}, within its interlayer spaces. This cation exchange capacity is a critical factor in its ability to adsorb and immobilize contaminants, including organic pollutants, heavy metals, and radionuclides [4]. Additionally, the clay's high surface area, often ranging from 700 to 800 m^2/g, provides extensive active sites for adsorption processes. One of the primary benefits of MMT is its effectiveness as an adsorbent in water and wastewater treatment [5]. The clay's high surface area and CEC facilitate the removal of organic pollutants, such as dyes and antibiotics, from aqueous solutions [6,7]. Furthermore, the ability of MMT to swell and disperse in water enhances its contact with pollutants, thereby improving adsorption efficiency. This characteristic is particularly advantageous in treating industrial effluents, where it can reduce the concentration of hazardous substances to acceptable levels. Beyond environmental applications, MMT clay is employed in a variety of fields. In the pharmaceutical industry, it serves as a drug delivery vehicle due to its biocompatibility and ability to intercalate active pharmaceutical ingredients [8]. Its role in cosmetics is also notable, where it functions as a base for creams and lotions, and is advantageous for its ability to adsorb oils and impurities from the skin [9]. Additionally, use of MMT in agriculture, as a soil conditioner and carrier for fertilizers and pesticides, underscores its multifunctional nature [10]. Moreover, both the thermal stability and chemical inertness of MMT make it an excellent candidate for use in polymer nanocomposites, enhancing the mechanical properties and thermal resistance of resulting materials. Its incorporation into such composites can lead to significant improvements in material performance, broadening its applicability in advanced engineering and material science domains [11]. The distinctive structural properties and versatile functionality of MMT render it an invaluable material across multiple applications. Its effectiveness in adsorbing contaminants, coupled with its utility in pharmaceuticals, cosmetics, agriculture, and nanocomposites, highlight its broad potential and underscore the importance of ongoing research into optimizing its various uses. As mentioned above, layered silicates are able to form organoclay materials through the exchange of inorganic cations compensating the negative charge of silicates occurring both in the interlayers and on the outer particle surfaces. Typically, ammonium cations with longer alkyl chains or aromatic moieties have been used for the hydrophobic modification of layered silicates [12]. Organic cations containing diverse polar functionalities can provide organo-clay minerals with enhanced affinity for particular organic molecules such as pesticides [13].

Cationic polymers represent an alternative way for clay mineral modification. The polymer molar mass and the molar fraction of cationic units have been identified as important parameters for modification efficiency [14]. Polycation-modified clay minerals have been extensively studied as catalysts [15] or adsorbents for organic pollutants [16]. Similarly, naturally occurring polycation spermine with repeating propylene imine units was used, showing pronounced affinity for herbicides like fluometuron or diuron [17]. Clay minerals have also been modified with other synthetic and natural polycations such as cationic starch or chitosan mainly to produce nanocomposites with various polymeric matrices [18].

It was already stated that clay minerals are, due to their high specific surface areas, good adsorbents of various organic molecules, e.g. pesticides, air and water pollutants, metabolites or drugs [19]. In recent years, the removal of organic pollutants, including dyes and antibiotics, from aqueous solutions such as wastewater, has become a critical focus of environmental engineering and science [6,7]. These pollutants pose significant risks to aquatic ecosystems and human health due to their persistence and toxicity. Consequently, a variety of methods have been developed and optimized to address this pressing issue, each offering

distinct mechanisms and efficiencies. Adsorption methods, particularly those utilizing activated carbon, zeolites, and biomass-derived adsorbents, are widely employed due to their high surface areas and effectiveness in capturing a broad spectrum of organic contaminants [20]. Advanced oxidation processes, including photocatalysis, Fenton reactions, and ozonation, leverage reactive oxygen species in order to degrade complex organic molecules, demonstrating high efficacy albeit with potential cost and handling challenges [21]. Membrane filtration techniques such as nanofiltration, ultrafiltration, and reverse osmosis are highly efficient at removing organic pollutants, although they are often limited by membrane fouling and significant energy requirements [22]. Biological treatments harness the metabolic activities of microorganisms and plants in systems like activated sludge processes, constructed wetlands, and bioaugmentation, offering sustainable and cost-effective solutions, though sometimes at the expense of complete pollutant degradation rates [23]. Chemical treatments, including coagulation, flocculation, and chemical precipitation, provide efficient pollutant removal through the formation of easily removable aggregates or precipitates, but can introduce secondary contaminants [24]. Electrochemical methods, such as electrocoagulation and electrooxidation, utilize electric currents to induce pollutant removal reactions, combining versatility with high efficiency, yet often demanding substantial energy inputs [25]. Ion exchange techniques employ synthetic resins or natural materials like zeolites to selectively remove ions, offering high specificity and effectiveness, albeit with the challenge of managing waste brine [26]. Additionally, photolysis, both direct and sensitized, uses UV light to degrade pollutants directly or via reactive intermediates, presenting a straightforward but sometimes incomplete solution [27]. Hybrid methods that integrate multiple techniques have emerged to capitalize on the strengths of each approach, enhancing overall treatment efficiency. Examples include combining adsorption with photocatalysis or integrating biological treatments with membrane filtration [28]. Each of these methods presents unique advantages and limitations, necessitating a careful selection based on the specific pollutants involved, economic feasibility, and environmental impact [29]. From the wide group of hazardous chemicals, CBRN (C - chemical, B - biological, R - radioactive, and N - nuclear) agents pose a significant security threat in military conflicts, terrorist attacks, and industrial accidents. Protection against them is therefore a key societal priority. Comprehensive protection strategies are multi-faceted and include organizational measures, monitoring and analytics, barrier protection, external decontamination means, and antidotes for internal exposure. Therefore, the development of self-decontaminating materials capable of inactivating CBRN agents, whose adsorption and decontamination effects can target the surface of skin, clothing, articles of general consumption, or even objects used in public spaces, including means of transport and other technology in use, is of high importance.

In the case of chemical warfare agents (CWA), which fall under the CBRN category, their adsorption onto a suitable material, e.g. layered silicate-activated MMT (such as bentonite, a commercially available sorbent with the tradename Desprach), can be used as a preliminary strategy, but only leads to immobilization, as opposed to complete chemical destruction. The chemical decontamination of CWA is carried out by a reaction with suitable reagents that convert the CWA into nontoxic or less toxic products. Most commonly, mixtures containing active chlorine, most notably hypochlorites, oxidize a wide range of CWA [30]. Other (photo)oxidation processes have also been studied [31]. As most CWA are alkylating (yperite and its derivatives), acylating arsenic acid derivatives (Lewisite) or phosphorylating (organophosphates) agents, the use of suitable nucleophiles such as thiosulfate, British anti-Lewisite, amidoximes or oximes, or water with appropriate catalysis, is often an experimental strategy, however, each of these approaches has its drawbacks [32]. Enzymatic hydrolysis is sometimes too substrate-specific, as enzymes can be easily deactivated due to lability, and are also expensive [33]. Water-soluble metal complexes have relatively slow hydrolysis kinetics and unfavorable physicochemical properties, and can be costly for special ligands [34]. Metal-organic frameworks (MOFs) may have fast degradation kinetics, especially of organophosphates, but they are often unstable in moisture and complicated to handle [35]. Metal-oxide nanoparticles perform poorly in protic solvents and water [36]. Catalysts on imprinted polymers are complex and expensive to produce and too specific for a single CWA [37]. Catalytic efficiency can sometimes be improved for more hydrophobic CWA by micellar catalysis [38].

Water contamination by toxic organophosphates, such as paraoxon, poses significant environmental and health risks, necessitating effective remediation strategies. Clay minerals, particularly MMT, are promising adsorbents due to their high surface area, ion-exchange capacity, and tunable interlayer spacing. However, while pristine clays can efficiently adsorb contaminants, their limited ability to facilitate degradation presents a major challenge [39].

In the context of our study, cationic copolymers such as partially hydrolyzed poly(2-ethyl-2-oxazoline) (PEtOx-co-PEI) offer a means to enhance clay performance by improving dispersion, increasing surface charge, and modifying interlayer chemistry. These modifications can lead to improved contaminant uptake, better compatibility with biological environments, and, crucially, increased degradation rates of adsorbed toxins. Compared to conventional adsorbents like zeolites, resins, or functionalized silica, polymer-modified clays offer advantages in cost-effectiveness, scalability, and multifunctionality, combining adsorption with catalytic degradation. This study explores how such polymer-clay composites address key limitations in current remediation technologies and demonstrates their potential for environmental decontamination and biomedical applications.

Poly(2-oxazolines) represent versatile synthetic polymers suitable for different applications and bioapplications [40,41]. They can be prepared via living cationic polymerization, providing polymers with controlled molar mass, narrow dispersity, and different architecture [42]. Therefore, poly(2-oxazoline) can be used in (bio)applications requiring specific polymer size and topology. Moreover, poly(2-alkyl-2-oxazolines) have excellent *in vitro* performance, as exhibited by low cytotoxicity, no immunogenic effects and ultralow fouling of biofilm [43,44]. Poly(2-alkyl-2-oxazolines) with 2-methyl, 2-ethyl, and 2-propyl alkyl substituents have been used for the preparation of their statistical copolymers with poly(ethylene imine) through their partial hydrolysis [45–47]. In all cases, the degree of hydrolysis can be finely tuned by the concentration of used mineral acid, temperature, and time of hydrolysis. In previous work, we presented the effect of linear poly(2-oxazoline) and linear poly(ethylene imine) on the microstructure of modified MMT [48].

Herein, we report for the first time on the preparation of MMT modified with cationic polymers derived from poly(2-oxazolines), with the aim to decrease the negative cytotoxic effect of MMT. Poly(2-ethyl-2-oxazoline-co-ethylene imine)s containing a positive charge were prepared by the partial acidic hydrolysis of poly(2-ethyl-2-oxazoline). We compared *in vitro* cytotoxicity of cationic polymers containing different ratios of PEI units. Prepared copolymers were used for the organomodification of MMT, and their effect on the interlayer distance was studied. Selected organo-modified MMT was used for adsorption and the subsequent decontamination of paraoxon, which stands as a representative of organophosphate insecticides and warfare agents.

2. Experimental section/methods

2.1. Materials

Methyl 4-nitrobenzenesulfonate, hydrochloric acid, sodium chloride, dimethylsulfoxide (DMSO), 4-nitrophenol, 4-nitrophenyl phosphorodichloridate, triethylamine and lithium bromide were used as received from Sigma-Aldrich (Germany), and without further purification. Acetonitrile (Sigma -Aldrich, Germany) was dried and distilled over calcium hydride. 2-Ethyl-2-oxazoline (TCI Chemicals, Belgium) was

dried over potassium hydroxide for 48 h and distilled over calcium hydride under reduced pressure. Methanol (p.a.), absolute ethanol (p.a.) and potassium hydroxide were purchased from Mikrochem (Slovakia). N,N-dimethylacetamide (DMAc) suitable for HPLC, ≥ 99.9 % was purchased from Sigma-Aldrich (Germany). Deionized ultrapure water was obtained with Millipore (Direct-Q® 8 UV).

Homogenous solutions of previously synthesized and lyophilized poly(2-ethyl-2-oxazoline) and copolymers were prepared by dissolving 0.1 wt% of poly(2-ethyl-2-oxazolines) in a warm (50 °C) aqueous bath for 5 h. The smectite used in this study was reference montmorillonite Cheto, SAz-1 obtained from the Clay Minerals Society, Source Clay Repository (Department of Agronomy, Purdue University, West Lafayette, IN, USA).

2.2. Synthesis of paraoxon

The 4-nitrophenyl phosphorodichloridate (75.0 g, 293 mmol) was slowly added to anhydrous ethanol (500 mL) in a 1 L round-bottom flask. Under cooling and stirring, triethylamine (90 mL, 0.646 mmol) was slowly added through a septum, and after the last portion was added, the mixture was stirred for additional 2 h at room temperature. The mixture was then concentrated on a rotatory evaporator under reduced pressure and separated by extraction using water and diethyl ether layers. The diethyl ether layer was separated, concentrated on rotatory evaporator and as the residue still contained some triethylamine hydrochloride, it was again separated by extraction using water and diethyl ether. The diethyl ether layer was dried with anhydrous magnesium sulfate and evaporated, yielding 79.9 g (99 %) of the product. The purity was verified by thin-layer chromatography (TLC) using TLC Silica gel 60 F254 plates (Sigma-Aldrich, Germany). The retention factor (RF) of the product was 0.71 in diethyl ether as mobile phase.

^{1}H NMR (400.1 MHz, $CDCl_3$, δ, ppm): 8.17 (d, 2 H, Ar), 7.32 (d, 2 H, Ar), 4.18 (m, 4 H, CH_2), 1.30 (t, 6 H, CH_3). (see Figure S1 in the Supporting Information) ^{31}P NMR (100.6 MHz, $CDCl_3$, δ, ppm): −7.30 (see Figure S2 in the Supporting Information). ^{13}C NMR (100.6 MHz, CDCl3, δ, ppm): 155.64, 144.69, 125.72, 120.60, 65.22, 16.10 (see Figure S2 in the Supporting Information).

2.3. Preparation of poly(2-ethyl-2-oxazoline-co-ethylene imine)

In the first step, poly(2-ethyl-2-oxazoline) (PEtOx) was prepared by the cationic ring-opening polymerization of 2-ethyl-2-oxazoline initiated by methyl 4-nitrobenzenesulfonate according to the standard method [46]. Briefly, 10 mL (0.1 mol) of 2-ethyl-2-oxazoline and 0.22 g (0.001 mol) of methyl 4-nitrobenzenesulfonate were dissolved in 10 mL of dry acetonitrile (c = 4 mol•dm^{-3}) under an argon atmosphere to achieve the theoretical degree of polymerization equal to 100. The polymerization was performed at 80 °C for 48 h and terminated with 1.5 mL methanolic KOH (c = 0.1 mol•dm^{-3}) in 1.5-fold excess at ambient temperature for 2 h. The resulting polymer was purified by the dialysis toward deionized water (Spectra/Pro 6, MWCO 1000 Da, Spectrum Laboratories, USA). Yield: 9.1 g (91 %). M_n = 15,000 g•mol^{-1}. Đ = 1.19. The structure of the resulting polymer was confirmed by ^{1}H NMR spectrum (Figure S4). Then, poly(2-ethyl-2-oxazoline-co-ethylene imine) was prepared through the partial hydrolysis of PEtOx in 16.7 % hydrochloric acid as described elsewhere [46]. Briefly, 4.98 g of PEtOx was dissolved in 100 mL 16 wt% aqueous HCl and the solution was heated at 100 °C. 15 mL of the reaction mixture was withdrawn from the flask after 40, 60, 80, 120,180, and 240 min, cooled in liquid nitrogen and neutralized with 5 M aqueous KOH to pink color changes of dissolved phenolphthalein. The partially hydrolyzed polymer was purified by dialysis toward deionized water using dialysis membrane SpectraPro Nr.6 (MWCO 1 kDa, Spectrum Laboratories, USA) and then freeze dried. The degree of hydrolysis of all copolymers was determined from ^{1}H NMR spectrum (see Supporting Information, Figures S5-S10).

2.4. Preparation of modified clay minerals

The purified MMT fractions were obtained by dispersing 20 g of MMT lumps in 20 L of deionized water (0.1 % (w/v)) and were allowed to swell overnight and stirred (200 rpm) for 90 min. The supernatant slurry, having the desired clay particles size (<2 μm), was collected at a specific time (24 h) and height (21 cm) at room temperature (25 °C) and a precalculated time according to Stokes' law of sedimentation. The clay slurry obtained was Na-MMT saturated by repeated treatment with 1 M NaCl, and the < 2 μm fraction was collected. The excess of salt was removed by washing with deionized water until the $AgNO_3$ test for chlorides gave a negative result. The sample was dried at 60 °C and ground to pass a 0.2 mm sieve. The structural formula of the purified MMT calculated from the chemical analysis was $Na_{0.98}\ K_{0.02}\ Ca_{0.04}(Si_{7.98}\ Al_{0.02})(Al_{2.81}\ Fe_{0.13}\ Mg_{1.06})O_{20}(OH)_4$, and the cation exchange capacity (CEC) determined by the Cu–trien method was 1.21 mmol•g^{-1}.

For the preparation of PEtOx and PEtOx-*co*-PEI organoclays, the solvent intercalation process was used.

Sodium montmorillonite (Na-MMT, 200 mg) was added to 200 mL of distilled water and the suspension was stirred continuously for 24 h at a room temperature to ensure the Na-MMT was adequately exfoliated. Consequently, the calculated volumes (for each separate experiment) of 0.1 % aqueous solution of PEtOx or PEtOx-co-PEI were slowly (2 mL•min^{-1}) added to the stored suspension of Na-MMT under extensive stirring (900 rpm) at laboratory temperature (25 °C), and after the addition of the polymers, the mixture was continuously stirred for 10 days at 25 °C.

The content of PEtOx or PEtOx-co-PEI in the suspension was 50, 100, 250, and 500 mg PEtOx or PEtOx-co-PEI per 1 g of MMT.

After the reaction, the suspension was centrifuged, and the final product was washed (redispersed and centrifuged) three times with 200 mL of distilled water to remove excess of water-soluble polymer. Finally, the sample was quickly frozen and lyophilized at low pressure. The polymer–MMT nanocomposites obtained by this procedure are designated as Hx/*n*, where x denotes the level of PEtOx hydrolysis and *n* denotes the amount (in mg) of the poly(2-oxazoline) added to g of pure MMT.

For example:

H0/50 = 50 mg of PEtOx (batch H0) per 1 g MMT

H4/250 = 250 mg of PEtOx-co-PEI (batch H4) per 1 g MMT

2.5. Analytical methods

^{1} H NMR spectra were recorded at room temperature on a Varian VXR-400 (Varian, USA) in $CDCl_3$ solution using tetramethylsilane (TMS) as an internal standard. The concentration of (co)polymers was in all cases equal to 10 mg•mL^{-1}.

^{1}H NMR, ^{31}P NMR and ^{13}C NMR spectroscopy was used for paraoxon structural characterization. All spectra were acquired with a Bruker Avance NEO 400 spectrometer operating at: 400.1 MHz for ^{1}H, 161.9 MHz for ^{31}P and 100.6 MHz for ^{13}C at 299 K using $CDCl_3$ as a solvent. The acquisition parameters were as follows: for ^{1}H NMR, width of 90° pulse was 16.5 μs, relaxation delay 10 s, acquisition time 3.28 s and 32 scans; for ^{31}P NMR, width of 90° pulse was 10 μs, relaxation delay 15 s, acquisition time 0.46 s and 2000 scans; for ^{13}C NMR, width of 90° pulse was 10 μs, relaxation delay 10 s, acquisition time 1.18 s and 18000 scans.

Molar mass and dispersity of PEtOx were recorded by gel permeation chromatography (GPC) using DMAc with the addition of 0.1 wt% LiBr as an eluent. The GPC system consisted of a Shimadzu LC-20 pump (Shimadzu Corporation, Kyoto, Japan), Shimadzu refractive index detector (Shimadzu USA Manufacturer Inc., Canby, OR, USA) and two PPS PFG 5 μm columns or PSS GRAM 5 μm columns (Polymer Standard Services,

Mainz, Germany; d = 8 mm, l = 300 mm; 100 + 1000 Å) at 25 °C. Flow rate was set to 1 mL•min^{-1}. Poly(methylmethacrylate) (PMMA) standards (Polymer Standard Services, Mainz, Germany) were used for a calibration. Polymer concentration was 1 mg•mL^{-1} in DMAc.

X-ray diffraction (XRD) patterns were measured on X'Pert PRO (PANalytical B.V.) diffractometer equipped with CuKα (λα1 =1.54060 Å) radiation and operating at 45 kV 40 mA. The patterns were scanned in the 2θ range of 2–20°, with scanning step 0.026° 2θ and scan step time 100 s.

2.6. In vitro cytotoxicity of statistical copolymers and organo-modified montmorillonites

After thawing, the 3T3 fibroblasts (DSZM, Braunschweig, Germany) were cultured in Dulbecco-minimal essential medium (DMEM, Sigma-Aldrich, Germany) with 10 % FBS in a CO_2 incubator at 37°C, 5 % CO_2 with saturated humidity. Before the experiment, cells were collected by trypsinization using trypsine-EDTA (Gibco, BRL) for 1 min at room temperature and centrifuged at 1500 rpm for 3 minutes. The number of cells was determined using the Bürker chamber. Cells were seeded in a 96-well tissue-culture plate at a concentration of 5,000 cells per well in the culture medium and cultivated overnight. The next day polymers were dissolved and organo-modified MMT was dispersed in culture media in respective concentration ranges and applied to the cells. Polymers were incubated 24 h and 48 h and MMT 24 h. After the incubation time, solutions were removed, and cells treated with MMT were rinsed once with phosphate buffer solution (PBS, Sigma-Aldrich, Germany) to remove the clay, and a 3-(4,5-dimethyldiazol-2-yl)-2,5-diphenyl tetrazolium bromide (MTT, Sigma-Aldrich, Germany) dispersion with a concentration of 0.5 mg•mL^{-1} in culture media was added to the cells and incubated 3 h. Afterwards, the MTT dispersion was removed and 100 μL of DMSO was added to the wells. Optical density (OD) was determined at 595 nm.

2.7. Statistical analysis

Statistical analysis was performed by one-way ANOVA and post hoc Tukey test. Results were considered significant when differences equaled or exceeded the 95 % confidence level (* $p < 0.05$, ** $p < 0.01$ or *** $p < 0.001$).

2.8. Hydrolytic decomposition of paraoxon by organomodified montmorillonites

UV/Vis absorbance of 4-nitrophenol solutions with concentrations ranging from 0.001 to 0.4 mM was measured in aqueous 0.15 M Tris buffer at pH = 7.4 on a Varioskan LUX Multimode Microplate Reader (Thermo Fisher Scientific; Waltham, MA, USA). The blank sample consisted of Tris buffer only, all measurements were performed at room temperature in triplicate, and the optical absorbance at 400 nm wavelength was plotted as a UV-Vis calibration line of 4-nitrophenol.

The second step consisted of the preparation of 1 mM paraoxon solution with 0.05 wt% of neat or polymer-modified MMT in Tris buffer (pH = 7.4), which was stirred in a reaction flask at 50°C. To determine the optical absorbance of the reaction mixture, its aliquots were taken after set periods of time, measurement was performed at room temperature as described above, and the remaining mixture was returned to the flask afterwards. Dispersed unmodified MMT, copolymer poly(2-ethyl-2-oxazoline-co-ethylene imine) (H6), and MMT modified by two different ratios of H6 in Tris (0.05 wt% of solute) served as blank samples of subtracted light scattering baseline (the same composition but without paraoxon).

2.9. Kinetical analysis of paraoxon adsorption on montmorillonites in aqueous solution

An exponential fit was used to determine if the kinetic data acquired in the presence of MMT can be described by the pseudo-first-order (PFO) model of paraoxon adsorption [49], given by Eq. (1).

$$q_t = q_e \cdot \left(1 - e^{-k_1 \cdot t}\right) \quad (1)$$

where q_t and q_e are the adsorption amounts of paraoxon on the clay particles at time t and at equilibrium time, respectively (mg/g), and k_1 is the adsorption rate constant (h^{-1}).

The values of adsorption amount q_t were calculated from Eq. (2).

$$q_t = \frac{V \bullet (C_0 - C_t)}{m} \quad (2)$$

where V is the volume of the solution (L); C_0 is the initial concentration of paraoxon (mg/L); C_t is the concentration of paraoxon remaining in the solution at time t after the beginning of adsorption (mg/L); m is the mass of the adsorbent (g).

3. Results and discussion

3.1. Synthesis and characterization of poly(2-ethyl-2-oxazoline-co-ethylene imine)s

Organic compounds containing positive charges are widely employed as efficient modifiers for intercalation of clay minerals, e.g. smectites or halloysites, through cation exchange in the interlayer space [13]. Cationic polymers represent a possible alternative for modification of clay minerals toward the formation of stable (nano)composites with a plethora of synthetic and natural polymers. Here, statistical copolymers of poly(2-ethyl-2-oxazoline) with poly(ethylene imine) were prepared in two-step synthesis consisting of the living cationic ring-opening polymerization (LCROP) of 2-ethyl-2-oxazoline and the subsequent partial hydrolysis of poly(2-ethyl-2-oxazoline) under acidic conditions according to the procedure described elsewhere (Fig. 1) [46].

LCROP of 2-ethyl-2-oxazoline was performed in acetonitrile using methyl 4-nitrobenzenesulfonate as an initiator. Polymerization proceeded in 91 % yield. The molar mass of the resulting PEtOx as calculated from gel permeation chromatography (GPC) was 15000 g•mol^{-1}, which was slightly higher than the theoretical value, and the dispersity was equal to 1.19. The chemical structure was determined by ^{1}H NMR (Figure S2, Supporting Information)

Acidic hydrolysis was performed in 16.7 wt% aqueous HCl at 100°C in different time intervals. The molar fraction of ethylene imine units was determined from ^{1}H NMR and calculated values gradually increased with the increasing time of hydrolysis (Figures S5-S10, Supporting information). The rate of hydrolysis performed at 100 °C was equal to 5.9×10^{-5} s^1 according to kinetics of the first order (Fig. 2). The composition of the statistical copolymers formed in the second step was driven by the different times of hydrolysis as can be seen from Table 1. We expect that partial hydrolysis of poly(2-ethyl-2-oxazoline) provides copolymers with fully random distribution of N-propionyl-ethyleneimine and ethyleneimine units. The sequence analysis of partially hydrolyzed poly(2-ethyl-2-oxazolines) provided by bulk mass spectroscopy described in the work of Morgan et al. revealed the stochastic character of acidic hydrolysis. This indicates that ethyleneimine unit distribution corresponded to a theoretically modeled random distribution [50].

The residual charge of statistical copolymers was characterized by the zeta potential measurements. The zeta potential values listed in Table 1 clearly indicate that a positive charge was found for copolymers with an ethylene imine content higher than 22 mol% units.

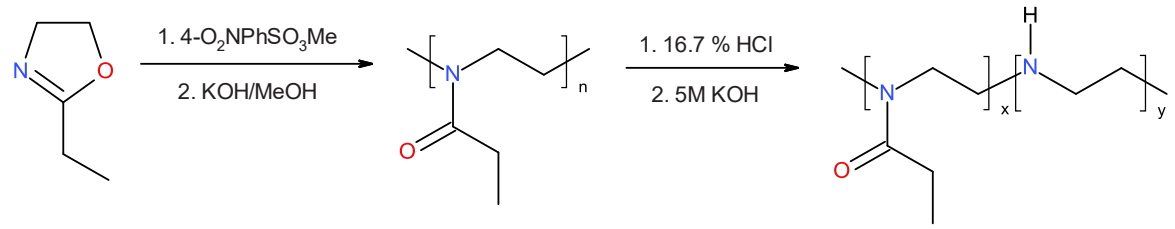

Fig. 1. Scheme of synthesis of poly(2-ethyl-2-oxazoline-co-ethylene imine).

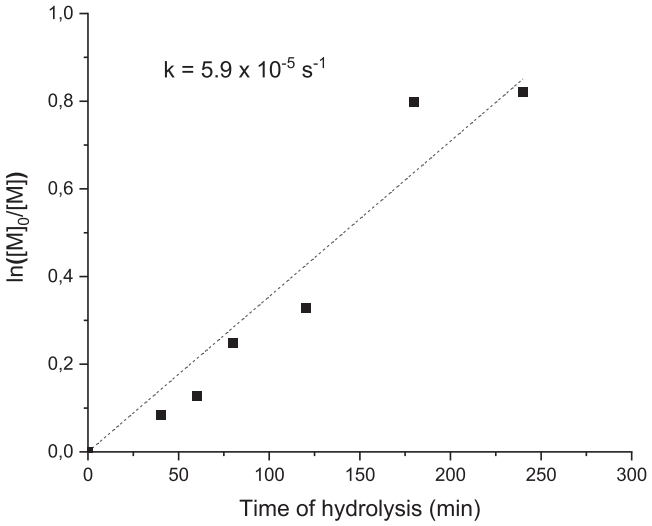

Fig. 2. Kinetic plot of the hydrolysis of poly(2-ethyl-2-oxazoline).

Table 1
The molar fractions and zeta potential of resulted poly(2-ethyl-2-oxazoline-co-ethylene imine)s.

Sample	H1	H2	H3	H4	H5	H6
Time of hydrolysis [min]	40	60	80	120	180	240
Degree of hydrolysis [mol%]	9	12	22	28	55	56
Zeta potential [mV]	0 ± 0	−1,2 ± 0,1	+ 1,6 ± 0,2	+ 16,6 ± 0,7	+ 25,7 ± 0,4	+ 29,7 ± 0,4

3.2. Modification of montmorillonites with poly(2-ethyl-2-oxazoline-co-ethylene imine)s

Prepared statistical copolymers PEtOx-co-PEI were used to compensate for the negative charge of MMT layers. Organoclays were prepared by the intercalation of different copolymer amounts per 1 g of MMT. The XRD patterns of the powder samples of PEtOx-co-PEI organoclays were analyzed in order to evaluate the impact of the initial concentration of copolymers, used for the sample preparation, on the changes in basal spacing value (d_{001}), reflecting the expansion of the interlayer space (Table 2). The initial modification carried out with 50 mg of PEtOx (sample H0) caused only minimal changes in d_{001} position (pure Na-MMT has 12.4 Å). However, a slight broadening of the *001* reflection was observed, therefore the incorporation of the polymer at a small extent was noticed. Using 100 mg of PEtOx per 1 g of MMT resulted in pronounced broadening of a diffraction peak and shift of the reflection maxima to a lower angle with a basal spacing of 13.17 Å. The increase of the PEtOx concentration in H0–100 caused more pronounced uniform distribution of the *001* reflection, with an approximate shift of

Table 2
d_{001} values [in Å] of the basal spacing for montmorillonites (MMT) modified with various statistical copolymers PEtOx-co-PEI from 50 mg copolymer per 1 g MMT to 500 mg copolymer per 1 g MMT.

	50	100	250	500
H0	12.73	13.17	20.47	21.24
H1	12.78	12.92	20.59	21.64
H2	12.78	12.82	20.35	21.24
H3	12.97	13.17	19.64	20.98
H4	13.22	13.98	17.79	20.85
H5	13.22	13.87	15.24	17.98
H6	13.07	14.04	16.03	18.27

0.8 Å to a lower *d*-value compared to Na-MMT. This observation refers to the prevalent monolayer arrangement of polymer chains in the interlayer space. The unexpected impact on layer stacking of prepared nanocomposites was observed with additional loading of the PEtOx polymer. A doubling of the polymer concentration (250 mg) caused a significant change of the d_{001} value to 20.47 Å, indicating a dominant bilayer arrangement at this concentration of polymer. Continued increase of polymer loading affected the distance between the layers, and the d_{001} value increased to 21.24 Å for H0–500. A basal spacing of the samples prepared with 250 and 500 mg of PEtOx indicated the creation of polymer double layers or possibly also a *pseudo*-trilayer arrangement in MMT interlayers.

Intercalates prepared with PEtOx-co-PEI copolymer showed similar but less pronounced trends. As the content of PEI in the copolymer increased, the interlayer expansion of the prepared organoclay decreased, for example in the case of the H5–500 sample with the highest content of PEI fraction, the d_{001} value was equal to 17.98 Å, roughly 3.25 Å less than in the case of H0–500. Generally speaking, the expansion of the clay interlayers was diminished as the content of PEI in copolymers increased. Thus, XRD consistently shows that these samples are in a hybrid structure where intercalated silicate layers coexist in considerable ratios.

In this study, PEtOx-co-PEI co-polymers were water soluble and the smectite layers were swelled in solvent. In the first stage, the layered silicate was swollen in water and then the polymer chains intercalated and displaced the solvent within the interlayer of MMT during the mixing of the polymer solutions and layered aluminosilicate dispersion. After solvent removal, the intercalated structure remained and the result was a nanocomposite. In terms of thermodynamics, a negative variation in the Gibbs free energy is required for the overall process, in which the polymer is exchanged with the previously intercalated solvent in the gallery. The entropy obtained by desorption of solvent molecules is the driving force for the polymer intercalation into layered smectite from a solution, which compensates for the decreased entropy of the confined, intercalated chains [51].

Fig. 3 displays the dependence of the zeta potential on the type of copolymer and the degree of loading in organo-modified MMT. These results show that the negative charge of MMT was fully compensated only in the case of PEtOx-co-PEI with 55 mol% PI (H5) and PEtOx-co-PEI with 56 mol% PI (H6), respectively, using the highest content of copolymer in the organoclay (H5–500 and H6–500).

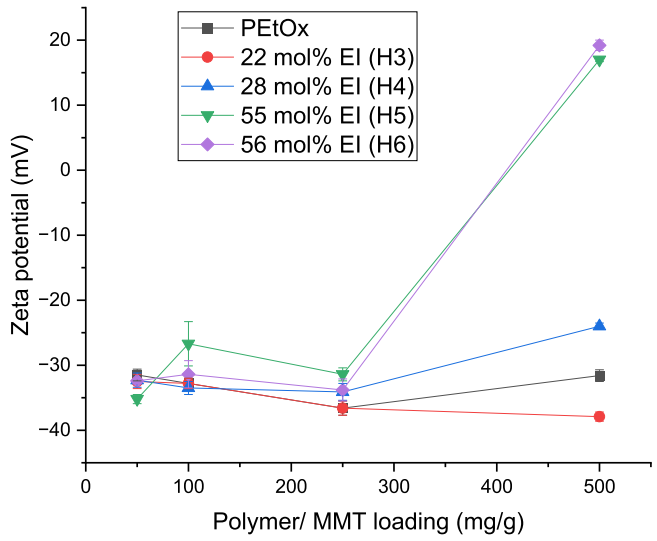

Fig. 3. Dependence of zeta potential of organo-modified MMT on the (PETOx-co-PEI) composition and a loading of copolymer in the organoclay.

3.3. *In vitro cytotoxicity studies of copolymers and organoclays*

In vitro cytotoxicity of PEtOx and its partially hydrolyzed copolymers was evaluated using 3T3 mice fibroblasts. The effect of hydrolysis and the content of EI on cell viability was determined after 24 and 48 h of incubation. With an increased degree of hydrolysis (increased content of EI), the cytotoxicity of copolymers increased (Fig. 4), as was also demonstrated in previous studies [46]. We reported previously that *in vitro* cytotoxicity is dependent not only on the polymer type and concentration, but also on the type of cells. 3T3 fibroblasts were found to be less sensitive than other cell lines [46].

Copolymers PEtOx-co-PEI with EI content of 22 mol% (H3) are considered non-cytotoxic up to a concentration of 20 mg•mL^{-1} with cell viability above 70 %. Copolymers containing 28 mol% and 55 mol% of EI units (H5) are non-cytotoxic only up to a concentration of 5 mg•mL^{-1} or lower than 1 mg•mL^{-1}, respectively.

To evaluate the *in vitro* cytotoxicity of polymers, it is also important to observe the change in the morphology of the cells after their treatment with the tested samples. The typical morphology of fibroblasts is spindle- or branched-shaped cells with an oval nucleus, as can be seen in the control cells in Figure S11 (Supporting Information). After the treatment of cells with PEtOx, no changes in morphology were observed. In the case of PEtOx-co-PEI 22 mol% (H3), no changes in morphology were observed, except at the highest concentration of 20 mg•mL^{-1} where some cells lost typical spindle-shape morphology, and became round with the presence of apoptotic bodies. With increasing content of EI units, e.g. in the PEtOx-co-PEI 55 mol% (H5), the apoptotic cells appeared also at lower concentrations. The effect of time is best noticeable by H5 at a concentration of 20 mg•mL^{-1} where after 24 h, both living and apoptotic cells were visible, but after 48 h were mostly dead and apoptotic cells were observed, similar to positive control PEI at a concentration of 10 mg•mL^{-1} (Figure S12, Supporting Information).

This work aimed to prepare MMT with improved adsorption capability and biocompatibility for use in biomedicine and other applications where contact with the human body occurs. It was shown previously using different cell lines that MMT reduces cell viability with respect to concentration and cell line used [52]. As expected, the non-modified MMT used in this study significantly decreased the viability of 3T3 mouse fibroblasts, which was less than 20 % at concentrations higher than 5 mg•mL^{-1} (Figure S13, Supporting Information). The cytotoxic effect can be reduced through different modifications of clays [53]. For example, the modification of MMT with oligo(styrene-co-acrylonitrile) increased the viability of NIH-3T3 and HEK 293 cells [54]. There are several studies where poly(lactic-co-glycolic acid)-modified clays, such as Laponite or Halloysite, increased cell viability several times over when used for scaffold formation in bone regeneration and tissue engineering [55–58]. Thus, the modification of MMT with non-cytotoxc PEtOx and PEtOx-co-PEI was expected to improve their biocompatibility. Therefore, three different (co)polymers were selected: PEtOx as a non-ionic polymer, and two copolymers carrying a cationic charge with 22 mol% (H3) and 55 mol% (H5) of EI units. There were four different PEtOx-co-PEI/MMT loadings used: 50, 100, 250, and 500 mg per 1 g of MMT. Organo-modification of MMT with PEtOx significantly improved biocompatibility using 100 mg per 1 g MMT and higher (Fig. 5a). Loading of PEtOx equal to 500 mg/g increased cell viability 3.5 times at the highest concentration (10 mg•mL^{-1}) compared to pure MMT. The modification of MMT with H3 had a similar effect on cell viability, where the loading of 500 mg per 1 g at the highest concentration increased cell viability 5.5 times as compared to pure MMT (Fig. 5b). Use of the copolymer with 55 mol% of EI units (H5) also led to significantly improved biocompatibility, showing a 3.5 times increased viability similarly to PEtOx-modified MMT (Fig. 5c).

The positive effect of (co)polymer-modified MMT is also supported by the morphological analysis of cells. Generally, with increased saturation of MMT with the (co)polymer from 50 to 500 mg•g^{-1}, the number of apoptotic cells decreased and fibroblasts maintained their typical spindle- or branched-shaped morphology (Figure S11, see Supporting Information). On the other hand, the non-modified MMT had a visibly negative effect on cell morphology with increasing concentration.

Thus, we conclude that the cytotoxic effect of non-modified MMT can be reduced by the organo-modification with PEtOx and PEtOx-co-PEI containing 22 mol% and 55 mol% of EI units when the loading of (co)polymer is equal to 100 mg/g or higher. With increasing loading of (co)polymers in MMT up to 500 mg•g^{-1} we can diminish the *in vitro* cytotoxic effect of MMT. The poly(2-oxazolines) and their copolymers are known for their non-cytotoxicity and as drug and gene delivery vehicles [59]. The presented novel type of poly(2-oxazoline)- modified MMT has a high potential in its utilization as a drug delivery system in biomedical applications.

3.4. *Sorption and decomposition of paraoxon in the presence of organo-modified montmorillonites*

As previously stated, absorbents based on smectites are widely used for adsorption of different pollutants including pesticides, drugs or metabolites. Here we demonstrated both efficient adsorption and, importantly, the following deactivation properties of organo-modified MMT towards the neurotoxic organophosphate paraoxon. Paraoxon is a parasympathomimetic agent which acts as a cholinesterase inhibitor [60]. Paraoxon was also used as an ophthalmological drug against glaucoma. Paraoxon is one of the most potent organophosphate-based acetylcholinesterase-inhibiting insecticides available on the market, and is thus now only rarely used as an insecticide due to the risk of poisoning to humans and other animals. Paraoxon has been studied in regards to both the acute and chronic effects of organophosphate intoxication [61]. It is easily absorbed through skin, and was allegedly used as an assassination weapon by the apartheid-era South African chemical weapons program, Project Coast [62]. Paraoxon can be decomposed by basic, metal-catalyzed, or enzymatic hydrolyses (Fig. 6) and is often used as a model organophosphate as its hydrolysis is easy to follow by UV–VIS spectrophotometry [63–65]. In cases of basic hydrolysis, different amines have been used [66].

Here, paraoxon as an organophosphate model compound was synthesized from 4-nitrophenyl phosphorodichloridate with ethanol and triethylamine according to a procedure previously described in the literature [67]. The chemical structure of the prepared paraoxon was supported by ^{1}H, ^{13}C, and ^{31}P NMR spectra (see Supporting Information, Figures S12-S14).

Here, the kinetics of the paraoxon hydrolysis were evaluated using

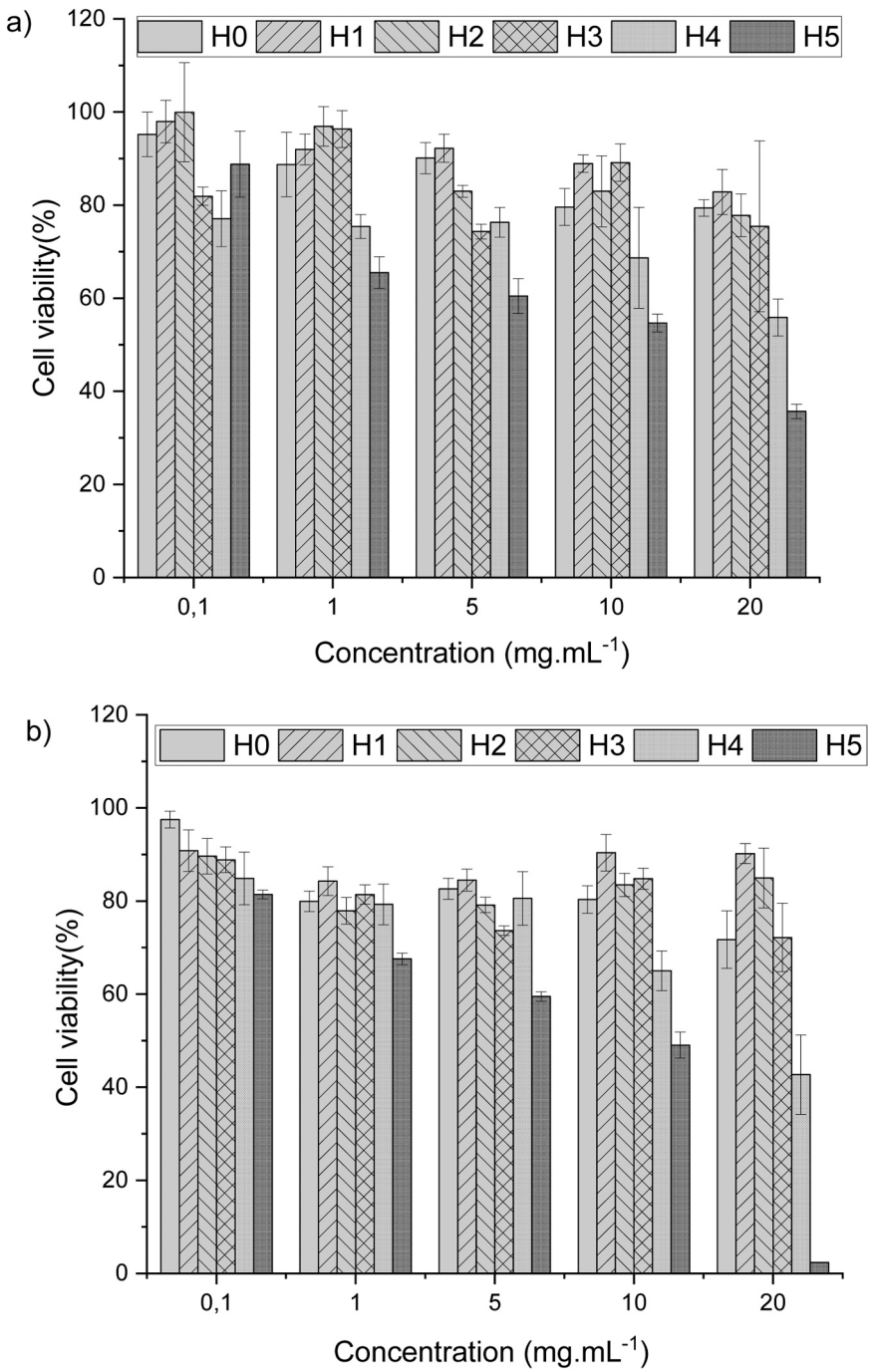

Fig. 4. *In vitro* cytotoxicity of PEtOx and copolymers PEtOx-co-PEI with various content of PEI on 3T3 fibroblasts after 24 h (a) and 48 h (b).

UV-Vis spectroscopy, and the signal of its decomposition product 4-nitrophenol was selected. 4-nitrophenol has a different spectrum than the original paraoxon, namely, the paraoxon does not absorb at all at 400 nm, where the 4-nitrophenolate exhibits strong absorption (see Supporting information, Figure S15 for calibration curve, Figure S16 for UV spectra).

To determine the hydrolytic activity of organo-modified clays against paraoxon, the dispersions of pristine or polymer-modified MMT in Tris buffer (pH = 7.4) with 1 mM paraoxon were taken after set periods of time, measurement was performed at room temperature, and the remaining mixture was returned to the flask afterwards (see Supporting information, Figure S17 for illustrative image). Dispersed non-modified MMT, copolymer poly(2-ethyl-2-oxazoline-co-ethylene imine) containing 56 mol% EI (H6), and MMT modified by two different ratios of H6 in Tris (0.05 wt% of solute) served as blank samples to subtract light scattering baseline (i.e., the same composition but without paraoxon). We observed that samples with MMT showed a sharp increase of absorbance after 5 min of stirring at 50 °C, which continued for 2 h. After that, absorbance quickly decreased and started to grow slightly with time. This behavior can be explained by the swelling of clay particles, leading to their disintegration into smaller ones, which absorbed the light less than the initial particles. The optical absorbance was plotted versus time (Fig. 7) and analyzed by the first order kinetics model (Fig. 8, Table 3).

The hydrolysis of paraoxon on non-modified MMT was very significantly slower than the spontaneous hydrolysis of pure paraoxon in buffer (PP), showing that MMT strongly adsorbs paraoxon, but also efficiently stabilizes it against hydrolysis after adsorption. Modification

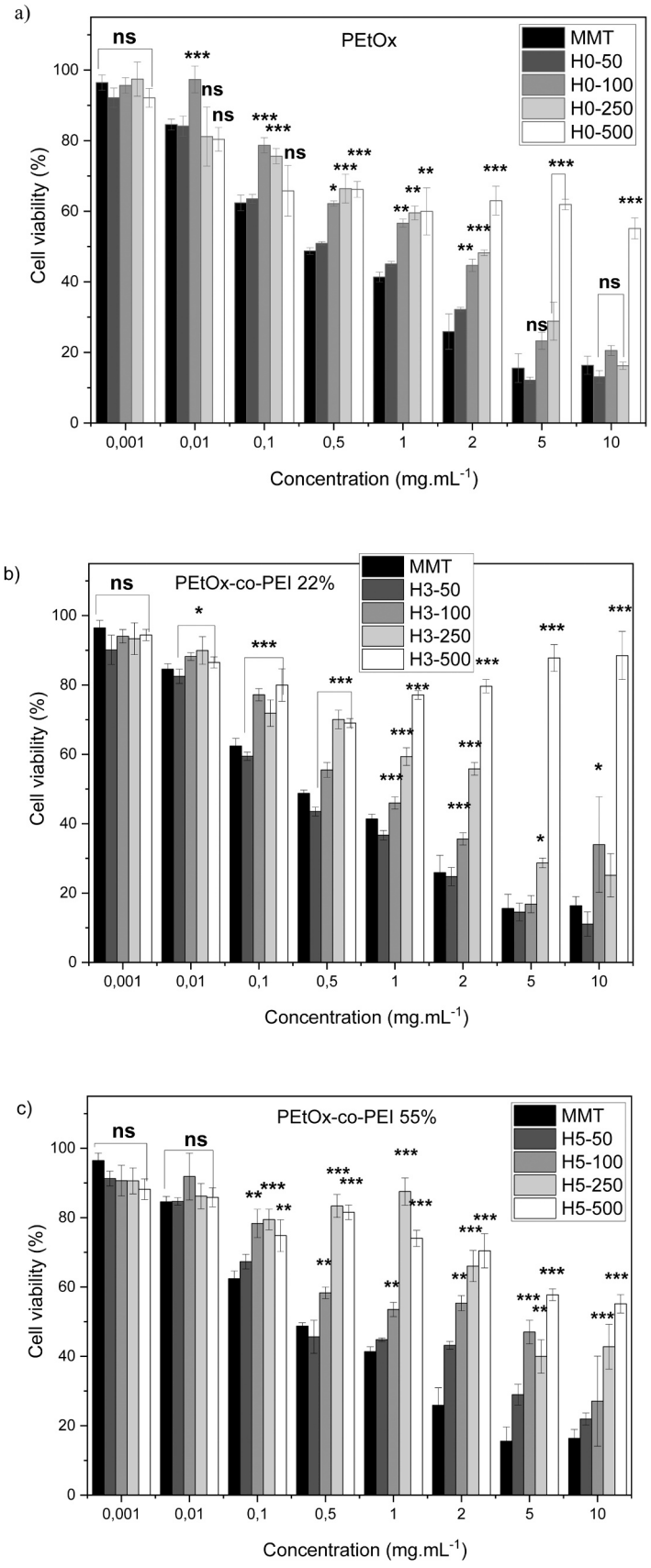

Fig. 5. Cell viability of non-modified MMT and MMT modified with PEtOx(a), PEtOx-co-PEI with 22 mol% EI (H3) (b), and PEtOx-co-PEI with 55 mol% EI (H5) (c). For each copolymer, four different loadings were used (50, 100, 250, and 500 mg•g^{-1}). Statistical analysis was performed by one-way ANOVA and post hoc Tukey test and results were considered significant when differences equaled or exceeded the 95 % confidence level (* $p < 0.05$, ** $p < 0.01$ or *** $p < 0.001$) or not-significant (ns).

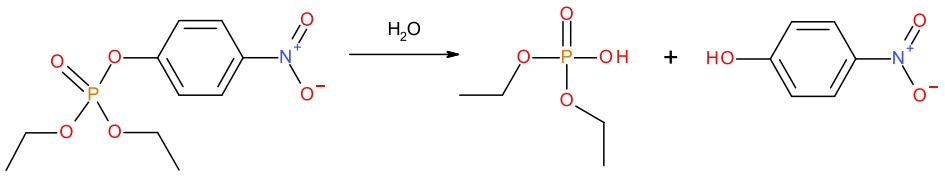

Fig. 6. Scheme of hydrolytic degradation of paraoxon.

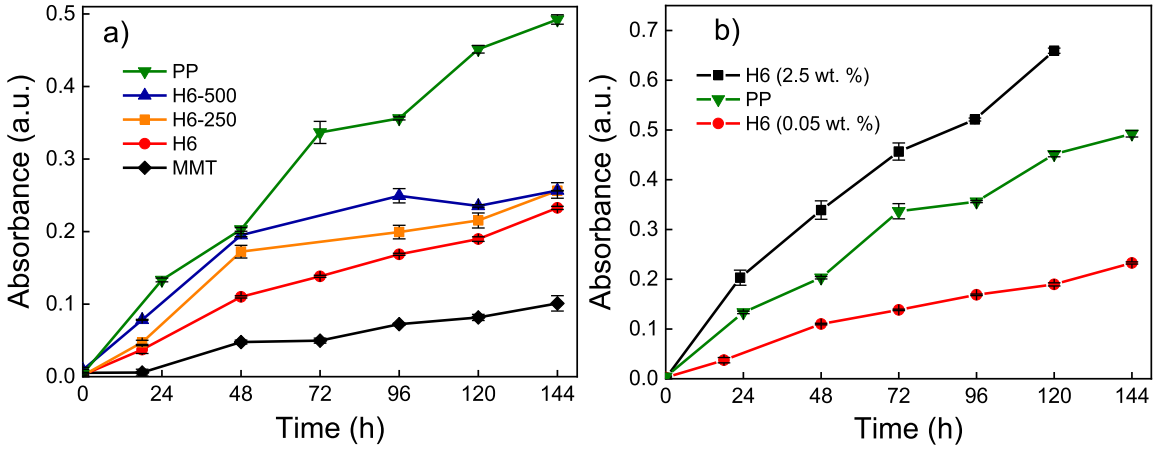

Fig. 7. Temporal evolution of optical absorbance of 1 mM paraoxon solution in 0.05 wt% (a) and 0.05 + 2.5 wt% (b) of analyzed samples in Tris buffer at pH 7.4. PP – pure 1 mM paraoxon solution in Tris buffer.

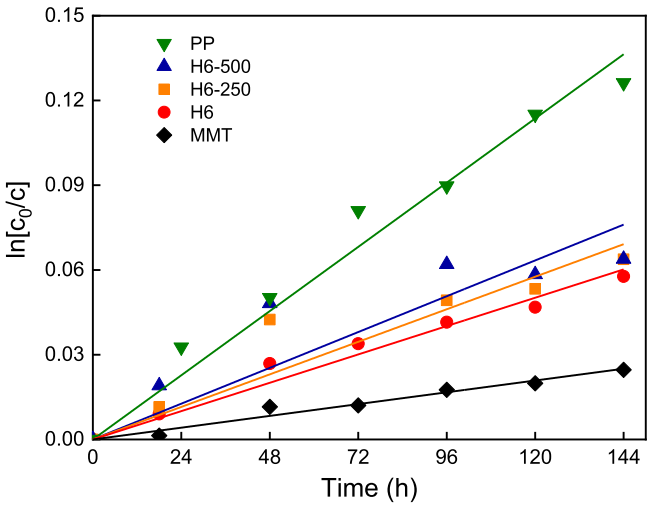

Fig. 8. First-order kinetic plots of paraoxon hydrolysis in pre-incubated 0.05 wt % dispersions of organo-modified MMT in Tris buffer at pH 7.4 compared to hydrolysis of pure 1 mM paraoxon solution in Tris buffer (PP) and in the presence of 0.05 wt% H6 dissolved in Tris buffer at pH 7.4.

of MMT with the soluble partially hydrolyzed poly(2-ethyl-2-oxazoline) H6 significantly increased the hydrolysis rate of paraoxon compared to non-modified MMT. The hydrolysis rate on less (H6–250) and more (H6–500) modified MMT is similar, and was somehow faster for the more modified MMT H6–500. Interestingly, H6 itself without MMT was weakly inhibitory for paraoxon hydrolysis at a low concentration 0.05 % against PP control, but catalytic at a higher concentration 2.5 %, showing that the catalysis mechanism may involve cooperative interactions existing in more concentrated polymer solution or on the surface of polymer-coated MMT, but not in diluted polymer solution (Fig. 9, Table 4).

As polymer-modified MMT in its exfoliated form in water is essentially composed of anionic silicate sheets coated with a layer of cationic polymer polycations permeable for low molecular weight compounds, the most plausible mechanism is the adsorption of paraoxon on the silicate surface followed by the nucleophilic attack of water augmented by the basic nature of the adsorbed partially hydrolyzed polymer according the scheme displayed in Figure S18.

The results therefore pave the way for MMT-based nanoreactors for dephosphorylation reactions of neurotoxic organophosphate agents as the polymer modification of MMT switches pure adsorption to adsorption plus subsequent hydrolysis mode. Compared to other paraoxon decontamination methods, the performance of the polymer-modified MMT is intermediate, but it works at milder conditions, does not require additional technical treatment such as irradiation, and the polymer-modified MMT is also non-toxic.

The pseudo-first-order (PFO) fitting model according to the Eq. (1) resulted in the corresponding values of q_e and k_1 (Figure S19, Table S1). In the case of MMT, the determined error of both q_e and k_1 was almost the same as the values of these parameters, clearly indicating that the

Table 3
The first-order kinetic parameters of paraoxon hydrolysis in the presence of analyzed samples (0.05 wt%).

Sample	PP (pure paraoxon)	H6-500	H6-250	H6	MMT
R^2, coefficient of determination	0.968	0.738	0.861	0.968	0.969
Rate constant, h^{-1}	$(9.47 \pm 0.35)\cdot10^{-4}$	$(5.28 \pm 0.62)\cdot10^{-4}$	$(4.80 \pm 0.43)\cdot10^{-4}$	$(4.18 \pm 0.16)\cdot10^{-4}$	$(1.74 \pm 0.07)\cdot10^{-4}$
Half-life, h	732	1310	1445	1660	3980

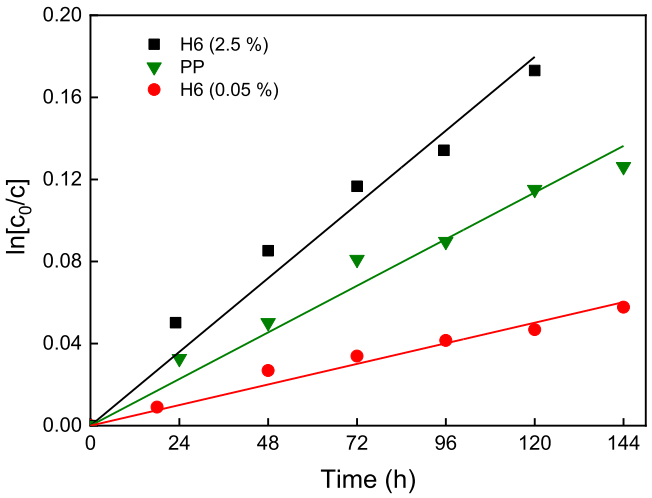

Fig. 9. First-order kinetic plots of paraoxon hydrolysis in presence of different concentrations of H6 dissolved in Tris buffer at pH 7.4. PP – pure 1 mM paraoxon solution in Tris buffer.

Table 4
The first-order kinetic parameters of paraoxon hydrolysis in presence of H6.

Sample	H6 (2.5 %)	PP (pure paraoxon)	H6 (0.05 %)
R^2, coefficient of determination	0.967	0.968	0.968
Rate constant, h^{-1}	(15.0 ± 0.63) x10^{-4}	(9.47 ± 0.35) x10^{-4}	(4.18 ± 0.16) x10^{-4}
Half-life, h	462	732	1660

PFO model was inapplicable. Thus, the pseudo-second-order (PSO) model of adsorption was tested, given by Eq. (3)

$$q_t = \frac{k_2 \bullet q_e^2 \bullet t}{1 + k_2 \bullet q_e \bullet t} \quad (3)$$

It produced a linear dependence in coordinates $1/q_t$ vs. $1/t$ (Figure S20), yielding the kinetic parameters q_e and k_2, which were presented in Table S2 [68]. But yet again, an unacceptably high error was generated by this model in the case of the H6–250 modified clay sample, implying that another mechanism could govern the adsorption kinetics.

Finally, the intraparticle diffusion (IPD) model was used with the Weber-Morris Eq. (4).

$$q_t = k_p \bullet t^{1/2} + C \quad (4)$$

where k_p was the intraparticle diffusion rate constant and C represented the particle boundary layer thickness. It was linearized in coordinates q_t vs. $t^{1/2}$, and its kinetic parameters were determined from the resulting linear fits (Figure S21 and Table S3). However, it was found to be inapplicable as well due to the obtained meaningless values of C, which were negative in the case of neat MMT and polymer-modified H6–250 clay.

The observed disparity between the experimental kinetic data and the theoretical adsorption models can be attributed to the fact that the chemical decomposition of paraoxon is the rate-determining step of the overall process, while the adsorption of paraoxon on the clay particles proceeded rather quickly. The latter may be the result of the low porosity of MMT, which has a layered structure, granting the easy access of adsorbate molecules to the particle surface.

The highest conversion of paraoxon into 4-nitrophenol during hydrolysis reached 15.90 % in the presence of H6 (2.5 wt%), while the lowest was 1.97 % with neat MMT (Table S4).

4. Conclusion

Statistic copolymers with various cationic capacity were prepared through partial hydrolysis of poly(2-ethyl-2-oxazoline). Hydrolysis proceeded via kinetics of the first order with the rate constant of 5.9x10^{-5} s^{-1}. In such manner, copolymers with six different molar fractions were prepared. We showed through zeta potential measurements that copolymers contain residual positive charge from a minimal molar fraction of 22 mol% of ethylene imine units. We demonstrated the non-cytotoxic character of statistical copolymers based on the partial hydrolysis of poly(2-ethyl-2-oxazoline) with 55 mol% of ethylene imine units up to a concentration of 1 mg•mL^{-1}.

Poly(2-ethyl-2-oxazoline-co-ethylene imine)s with a different content of ethylene imine units were used for the organo-modification of MMT. The XRD patterns showed the different impact of MMT modification on basal spacing d_{001} values dependently on (co)polymer composition and amount of (co)polymer loaded to MMT. For all (co) polymers, d_{001} values increased with increasing polymer loading. Moreover, d_{001} values decreased with increasing content of EI units. This observation is consistent with published results for the organo-modification of MMT with poly(2-methyl-2-oxazoline) and poly (ethylene imine) homopolymers [48]. The modification of MMT with poly(2-ethyl-2-oxazoline-co-ethylene imine)s led to significantly improved biocompatibility compared to non-modified MMT.

Paraoxon, as a representative of organophosphate insecticides and warfare agents, was used for the assessment of sorption and decontamination activity of neat and organo-modified MMT. The MMT modified to different extents with partially hydrolyzed poly(2-ethyl-2-oxazoline) caused the more rapid hydrolysis of paraoxon as compared to non-modified MMT, clearly showing the synergy of cationic copolymers and supporting clay. This indicates that MMT-based adsorbents also provide pronounced deactivation activity against neurotoxic organophosphate agents.

This study has shown preliminary proof of concept of the possible use of the studied material. Detailed kinetic study, which is beyond the scope of this particular article, would investigate the effect of variables such as temperature, contact time, pH, concentration of common anions and cations in the aqueous solution, adsorbent dose and pollutant concentration on the efficiency of the removal process.

CRediT authorship contribution statement

Zhoukovskaya Hanna: Methodology, Investigation. **Kučka Jan:** Methodology, Investigation. **Vetrík Miroslav:** Methodology, Investigation. **Hrubý Martin:** Writing – review & editing, Methodology. **Kronek Juraj:** Writing – review & editing, Writing – original draft, Methodology, Funding acquisition, Conceptualization. **Kroneková Zuzana:** Writing – review & editing, Writing – original draft, Methodology, Investigation, Funding acquisition. **Jankovič Ľuboš:** Writing – review & editing, Methodology, Investigation. **Mošková Zuzana:** Methodology, Investigation. **Minarčíková Alžbeta:** Methodology, Investigation.

Declaration of Competing Interest

The authors declare that they have no known competing financial interests or personal relationships that could have appeared to influence the work reported in this paper

Acknowledgements

Authors are thankful to the Slovak Research and Development Agency for their financial support in the projects APVV 19–0487 and APVV 23–0635. This work was also financially supported by Slovak Grant Agency VEGA in projects Nr. 2/0172/21 and 2/0170/24. M.H. thanks to the Czech Science Foundation (grant No. 21–01090S). The authors from the Institute of Macromolecular Chemistry CAS, thank the

Ministry of Education and Youth and Sports of the Czech Republic for their financial support (grants # LUAUS24272 and EATRIS CZ LM2023053). The authors thank Rafal Konefal for the NMR measurements of paraoxon.

Appendix A. Supporting information

Supplementary data associated with this article can be found in the online version at doi:10.1016/j.colsurfa.2025.136534.

Data availability

Data will be made available on request.

References

[1] R. Ganigar, G. Rytwo, Y. Gonen, A. Radian, Y.G. Mishael, Polymer–clay nanocomposites for the removal of trichlorophenol and trinitrophenol from water, in: Appl. Clay Sci., 49, 2010, pp. 311–316, https://doi.org/10.1016/j.clay.2010.06.015.

[2] E. Ruiz-Hitzky, A. van Meerbeek, Clay mineral– and organoclay–polymer nanocomposite, in: F. Bergaya, B.K.G. Theng, G. Lagaly (Eds.), Handbook of Clay Science, Developments in Clay Science, Vol. 1, Elsevier, 2006, pp. 583–621.

[3] M.E. Parolo, G.R. Pettinari, T.B. Musso, M.P. Sanchez-Izquierdo, L.G. Fernandez, Characterization of organo-modified bentonite sorbents: The effect of modification conditions on adsorption performance, Appl. Surf. Sci. 320 (2014) 356–363, https://doi.org/10.1016/j.apsusc.2014.09.105.

[4] P. Huang, A. Kazlauciunas, R. Menzel, L. Lin, Determining the Mechanism and Efficiency of Industrial Dye Adsorption through Facile Structural Control of Organo-montmorillonite Adsorbents, 31, ACS Appl. Mater. Interfaces 9 (2017) 26383–26391, https://doi.org/10.1021/acsami.7b08406.

[5] Z.U. Zango, A. Garba, Z.N. Garba, M.U. Zango, F. Usman, J.-W. Lim, Montmorillonite for Adsorption and Catalytic Elimination of Pollutants from Wastewater: A State-of-the-Arts Review, Sustainability 14 (2022) 16441, https://doi.org/10.3390/su142416441.

[6] M.E. Essington, J. Lee, Y. Seo, Adsorption of Antibiotics by Montmorillonite and Kaolinite, Soil Sci. Soc. Am. J. 74 (2010) 1577–1588, https://doi.org/10.2136/sssaj2009.0283.

[7] C.C. Wang, L.C. Juang, T.C. Hsu, C.K. Lee, J.F. Lee, F.C. Huang, Adsorption of basic dyes onto montmorillonite, J. Colloid Interface Sci. 273 (2004) 80–86, https://doi.org/10.1016/j.jcis.2003.12.028.

[8] S. Jayrajsinh, G. Shankar, Y.K. Agrawal, L. Bakre, Montmorillonite nanoclay as a multifaceted drug-delivery carrier: A review, J. Drug Deliv. Sci. Technol. 39 (2017), https://doi.org/10.1016/j.jddst.2017.03.023.

[9] C. Viseras, R. Sánchez-Espejo, R. Palumbo, N. Liccardi, F. Garcia-Villen, A. Borrego-Sanchez, M. Massaro, S. Riela, A. López-Galindo, Clays in Cosmetics and Personal-Care Products, Clays Clay Miner. 69 (2021) 561–575, https://doi.org/10.1007/s42860-021-00154-5.

[10] K.M. Manjaiah, R. Mukhopadhyay, R. Paul, S.C. Datta, P. Kumararaja, B. Sarkar (Eds.), Modified Clay and Zeolite Nanocomposite Materials, Elsevier, 2019, pp. 309–329, https://doi.org/10.1016/B978-0-12-814617-0.00008-6.

[11] R. Wang, H. Li, G. Ge, N. Dai, J. Rao, H. Ran, Y. Zhang, Montmorillonite-Based Two-Dimensional Nanocomposites: Preparation and Applications, Molecules 26 (2021) 2521–2545, https://doi.org/10.3390/molecules26092521.

[12] M.F. Brigatti, E. Galan, B.K. Theng, Structures and mineralogy of clay Minerals, in: F. Bergaya, B.K.G. Theng, G. Lagaly (Eds.), Handbook of Clay Science, Developments in Clay Science, 1, Elsevier, 2006, pp. 19–86.

[13] a) M. Cruz-Guzmán, R. Celis, M.C. Hermosín, J. Cornejo, Adsorption of the Herbicide Simazine by Montmorillonite Modified with Natural Organic Cations, Environ. Sci. Technol. 38 (2004) 180–186, https://doi.org/10.1021/es030057w;
b) M. Cruz-Guzmán, R. Celis, M.C. Hermosín, W.C. Koskinen, J. Cornejo, Adsorption of Pesticides from Water by Functionalized Organobentonites, J. Agric. Food Chem. 53 (2005) 7502–7511, https://doi.org/10.1021/jf058048p.

[14] F. Mabire, R. Audebert, C. Quivoron, Flocculation properties of some water-soluble cationic copolymers toward silica suspensions: A semiquantitative interpretation of the role of molecular weight and cationicity through a “patchwork” model, J. Colloid Interface Sci. 971(984) 120–136. https://doi.org/10.1016/0021-9797(84)90280-7.

[15] C. Breen, R. Watson, Acid-activated organoclays: preparation, characterisation and catalytic activity of polycation-treated bentonites, Appl. Clay Sci. 12 (1998) 479–494, https://doi.org/10.1016/S0169-1317(98)00006-4.

[16] a) C. Breen, R. Watson, Polycation-Exchanged Clays as Sorbents for Organic Pollutants: Influence of Layer Charge on Pollutant Sorption Capacity, J. Colloid Interface Sci. 208 (1998) 422–442, https://doi.org/10.1006/jcis.1998.5804;
b) G.J. Churchman, Formation of complexes between bentonite and different cationic polyelectrolytes and their use as sorbents for non-ionic and anionic pollutants, Appl. Clay Sci. 21 (2002) 177–189, https://doi.org/10.1016/S0169-1317(01)00099-0.

[17] a) B. Gámiz, R. Celis, M.C. Hermosín, J. Cornejo, C.T. Johnston, Preparation and characterization of spermine-exchanged montmorillonite and interaction with the herbicide fluometuron, Appl. Clay Sci. 58 (2012) 8–15, https://doi.org/10.1016/j.clay.2012.02.005;
b) B. Gámiz, R. Celis, M.C. Hermosín, J. Cornejo, Organoclays as Soil Amendments to Increase the Efficacy and Reduce the Environmental Impact of the Herbicide Fluometuron in Agricultural Soils, J. Agricul, Food Chem. 58 (2010) 7893–7901, https://doi.org/10.1021/jf100760s.

[18] S.F. Wang, L. Shen, Y.J. Tong, L. Chen, I.Y. Phang, P.Q. Lim, T.X. Liu, Biopolymer chitosan/montmorillonite nanocomposites: Preparation and characterization, Polym. Degrad. Stab. 90 (2005) 123–131, https://doi.org/10.1016/j.polymdegradstab.2005.03.001.

[19] F. Bergaya, G. Lagaly, General introduction: clays, clay minerals, and clay science, in: F. Bergaya, B.K.G. Theng, G. Lagaly (Eds.), Handbook of Clay Science, Elsevier, Amsterdam, 2006, pp. 1–18.

[20] N. Jiang, R. Shang, S.G.J. Heijman, L.C. Rietveld, High-silica zeolites for adsorption of organic micro-pollutants in water treatment: A review, Water Res. 144 (2018) 145–161, https://doi.org/10.1016/j.watres.2018.07.017.

[21] M.A. Sina, M. Mohsen, Advances in Fenton and Fenton Based Oxidation Processes for Industrial Effluent Contaminants Control-A Review, Int J. Environ. Sci. Nat. Res. 2 (4) (2017) 555594, https://doi.org/10.19080/IJESNR.2017.02.555594.

[22] J. Cevallos-Mendoza, C.G. Amorim, J.M. Rodríguez-Díaz, Montenegro, M.d.C.B.S. M. Removal of Contaminants from Water by Membrane Filtration: A Review, Membranes 12 (2022) 570, https://doi.org/10.3390/membranes12060570.

[23] S.S. Chan, K.S. Khoo, K.W. Chew, T.C. Ling, P.L. Show, Bioresour. Technol. 344 (2022) 126159, https://doi.org/10.1016/j.biortech.2021.126159.

[24] J.T. Alexander, F.I. Hai, M. Al-aboud Turki, Chemical coagulation-based processes for trace organic contaminant removal: Current state and future potential, J. Environ. Manag. 111 (2012) 195–207, https://doi.org/10.1016/j.jenvman.2012.07.023, https://doi.org/10.1016/j.jenvman.2012.07.023.

[25] G. Chen, Electrochemical technologies in wastewater treatment, Sep. Purif. Technol. 38 (1) (2004) 11–41, https://doi.org/10.1016/j.seppur.2003.10.006.

[26] A. Dąbrowski, Z. Hubicki, P. Podkościelny, E. Robens, Selective removal of the heavy metal ions from waters and industrial wastewaters by ion-exchange method, Chemosphere 56 (2) (2004) 91–106, https://doi.org/10.1016/j.chemosphere.2004.03.006.

[27] H.C. Yap, Y.L. Pang, S. Lim, A.Z. Abdullah, H.C. Ong, C.-H. Wu, A comprehensive review on state-of-the-art photo-, sono-, and sonophotocatalytic treatments to degrade emerging contaminants, Int. J. Environ. Sci. Technol. 16 (2019) 601–628, https://doi.org/10.1007/s13762-018-1961-y.

[28] K. Dhangar, M. Kumar, Tricks and tracks in removal of emerging contaminants from the wastewater through hybrid treatment systems: A review, Sci. Total Environ. 738 (2020) 140320, https://doi.org/10.1016/j.scitotenv.2020.140320.

[29] A.K. Avornyo, S.W. Hasan, F. Banat, C.V. Chrysikopoulos, Preparation, characterization, and applications of kaolin/kaolin-based composite membranes in oily wastewater treatment: Recent developments, challenges, and opportunities, J. Environ. Manag. 370 (2024) 122800, https://doi.org/10.1016/j.jenvman.2024.122800.

[30] S. Bjarnason, J. Mikler, I. Hill, C. Tenn, M. Garrett, N. Caddy, T.W. Sawyer, Comparison of selected skin decontaminant products and regimens against VX in domestic swine, Hum. Exp. Toxicol. 27 (2008) 253–261, https://doi.org/10.1177/0960327108090269.

[31] M. Silva, J. Baltrusaitis, Destruction of emerging organophosphate contaminants in wastewater using the heterogeneous iron-based photo-Fenton-like, Process, J. Hazard. Mater. Lett. 2 (2021) 100012, https://doi.org/10.1016/j.hazl.2020.100012.

[32] P. Janoš, O. Tokar, M. Došek, K. Mazanec, P. Ryšánek, M. Kormunda, J. Henych, P. Janoš, Jr., Amidoxime-functionalized bead cellulose for the decomposition of highly toxic organophosphates, RSC Advances, 11 (2021) 17976–17984. https://doi.org/10.1039/D1RA01125A.

[33] M. Thakur, I.L. Medintz, S.A. Walper, A. Scott, Enzymatic Bioremediation of Organophosphate Compounds - Progress and Remaining Challenges, Front. Bioeng. Biotech. 7 (2019) 289, https://doi.org/10.3389/fbioe.2019.00289.

[34] a) G. Feng, D. Natale, R. Prabaharan, J.C. Mareque-Rivas, N.H. Williams, Efficient Phosphodiester Binding and Cleavage by a Zn^{II} Complex Combining Hydrogen-Bonding Interactions and Double Lewis Acid Activation, Angew. Chem. Int. Ed. 45 (2006) 7056–7059, https://doi.org/10.1002/ange.200602532;
b) C. Liu, L. Wang, DNA hydrolytic cleavage catalyzed by synthetic multinuclear metallonucleases, Dalton Trans. (2009) 227–239, https://doi.org/10.1039/B811616D.

[35] a) S.Y. Moon, Y.Y. Liu, J.T. Hupp, O.K. Farha, Instantaneous Hydrolysis of Nerve-Agent Simulants with a Six-Connected Zirconium-Based, Met. –Org. Framew., Angew. Chem. Int. Ed. 54 (2015) 6795–6799, https://doi.org/10.1002/ange.201502155;
b) T. Islamoglu, M.A. Ortuno, E. Proussaloglou, A.J. Howarth, N.A. Vermeulen, A. Atilgan, A.M. Asiri, C.J. Cramer, O.K. Farha, Presence versus Proximity: The Role of Pendant Amines in the Catalytic Hydrolysis of a Nerve Agent Simulant, Angew. Chem. Int. Ed. 57 (2018) 1949–1953, https://doi.org/10.1002/anie.201712645;
c) J.B. DeCoste, G.W. Peterson, B.J. Schindler, K.L. Killops, M.A. Browe, J. J. Mahle, The effect of water adsorption on the structure of the carboxylate containing metal–organic frameworks Cu-BTC, Mg-MOF-74, and UiO-66, J, Mater. Chem. A 1 (2013) 11922–11931, https://doi.org/10.1039/c3ta12497e.

[36] E. Denet, M. Betzabeth Espina-Benitez, I. Pitault, T. Pollet, D. Blaha, M.-A. Bolzinger, V. Rodriguez-Nava, S. Briançon, Metal oxide nanoparticles for the decontamination of toxic chemical and biological compounds, Int. J. Pharm. 583 (2020) 119373, https://doi.org/10.1016/j.ijpharm.2020.119373.

[37] J. Pan, S. Liu, H. Jia, J. Yang, M. Qin, T. Zhou, Z. Chen, X. Jia, T. Guo, Rapid hydrolysis of nerve agent simulants by molecularly imprinted porous crosslinked

polymer incorporating mononuclear zinc(II)-picolinamine-amidoxime module, J. Cat. 380 (2019) 83–90, https://doi.org/10.1016/j.jcat.2019.10.023.
[38] J. Cabal, J. Míčová, K. Kuča, Kinetics of hydrolysis of organophosphate soman by cationic surfactant Resamin AE, J. Appl. Biomed. 8 (2010) 111–116, https://doi.org/10.2478/v10136-009-0009-5.
[39] A. Ahmadi, R. Foroutan, H. Esmaeili, S.J. Peighambardoust, S. Hemmati, B. Ramavandi, Montmorillonite clay/starch/$CoFe_2O_4$ nanocomposite as a superior functional material for uptake of cationic dye molecules from water and wastewater, Mater. Chem. Phys. 284 (2022) 126088, https://doi.org/10.1016/j.matchemphys.2022.126088.
[40] T. Lorson, M.M. Lübtow, E. Wegener, M.S. Haider, S. Borova, D. Nahm, R. Jordan, M. Sokolski-Papkov, A.V. Kabanov, R. Luxenhofer, Poly(2-oxazoline)s based biomaterials: A comprehensive and critical update, Biomaterials 178 (2018) 204–280, https://doi.org/10.1016/j.biomaterials.2018.05.022.
[41] R. Hoogenboom, The future of poly(2-oxazoline)s, Eur. Polym. J. 179 (2022) 111521, https://doi.org/10.1016/j.eurpolymj.2022.111521.
[42] S. Jana, R. Hoogenboom, Poly(2-oxazoline)s: a comprehensive overview of polymer structures and their physical properties—an update, Polym. Int. 71 (2022) 935–949, https://doi.org/10.1002/pi.6426.
[43] a) J. Kronek, Z. Kroneková, J. Lustoň, E. Paulovičová, L. Paulovičová, B. Mendrek, In vitro bio-immunological and cytotoxicity studies of poly(2-oxazolines, J. Mater. Sci. Mater. Med. 22 (2011) 1725–1734, https://doi.org/10.1007/s10856-011-4346-z;
b) J. Kronek, J. Lustoň, Z. Kroneková, E. Paulovičová, P. Farkaš, N. Petrenčíková, L. Paulovičová, I. Janigová, Synthesis and bioimmunological efficiency of poly(2-oxazolines) containing a free amino group, J. Mater. Sci. Mater. Med. 21 (2010) 879–886, https://doi.org/10.1007/s10856-009-3949-0.
[44] J. Kronek, E. Paulovičová, L. Paulovičová, Z. Kroneková, J. Lustoň. Immunomodulatory efficiency of poly(2-oxazolines), J. Mater. Sci. Mater. Med. 23 (2012) 1457–1464, https://doi.org/10.1007/s10856-012-4621-7.
[45] E. Haladjova, M. Smolíček, I. Ugrinova, D. Momekova, P. Shestakova, Z. Kroneková, J. Kronek, S. Rangelov, DNA delivery systems based on copolymers of poly (2-methyl-2-oxazoline) and polyethyleneimine: Effect of polyoxazoline moieties on the endo-lysosomal escape, J. Appl. Polym. Sci. 137 (2020) e49400, https://doi.org/10.1002/app.49400.
[46] R. Shah, Z. Kroneková, A. Záhoranová, L. Roller, N. Saha, P. Saha, J. Kronek, In vitro study of partially hydrolyzed poly(2-ethyl-2-oxazolines) as materials for biomedical applications, J. Mater. Sci. Mater. Med 26 (2015) 157, https://doi.org/10.1007/s10856-015-5485-4.
[47] M. Mees, E. Haladjova, D. Momekova, B. Momekov, P. Shestakova, Ch Tsvetanov, R. Hoogenboom, S. Rangelov, Partially Hydrolyzed Poly(n-propyl-2-oxazoline): Synthesis, Aqueous Solution Properties, and Preparation of Gene Delivery Systems, Biomacromolecules 17 (2016) 3580–3590, https://doi.org/10.1021/acs.biomac.6b01088.
[48] J. Madejová, M. Barlog, M. Slaný, S. Bashir, E. Scholtzová, D. Tunega, Ľ. Jankovič, Advanced materials based on montmorillonite modified with poly(ethylenimine) and poly(2-methyl-2-oxazoline): Experimental and DFT study, Coll. Surf. A. Physicochem. Eng. Asp. 659 (2023) 130784, https://doi.org/10.1016/j.colsurfa.2022.130784.
[49] Y. Chuang, J. Chen, J. Lu, L. Su, S.Y. Jiang, Y. Zhao, C.H. Lee, Z. Wu, H.D. Ruan, Sorption studies of Pb(II) onto montmorillonite clay, IOP Conf. Ser.: Earth Environ. Sci. 1087 (2022) 1207, https://doi.org/10.1088/1755-1315/1087/1/012007.
[50] T.E. Morgan, T.G. Floyd, B.P. Marzullo, C.A. Wootton, M.P. Barrow, A.W. T. Bristow, S. Perrier, P.B. O'Connor, Stochasticity of poly(2-oxazoline) oligomer hydrolysis determined by tandem mass spectrometry, Polym. Chem. 13 (2022) 4162–4169, https://doi.org/10.1039/D2PY00437B.
[51] R.A. Vaia, E.P. Gianellis, Polymer melt intercalation in organically-modified layered silicates: model predictions and experiment, Macromolecules 30 (1997) 8000–8009, https://doi.org/10.1021/ma9603488.
[52] S. Maisanaba, S. Pichardo, M. Puerto, D. Gutiérrez-Praena, A.M. Cameán, A. Jos, Toxicological evaluation of clay minerals and derived nanocomposites: A review, Environ. Res. 138 (2015) 233–254, https://doi.org/10.1016/j.envres.2014.12.024.
[53] S. Murugesan, T. Scheibel, Copolymer/clay nanocomposites for biomedical applications, Adv. Funct. Mater. 30 (2020) 1908101, https://doi.org/10.1002/adfm.201908101.
[54] Q. Liu, Y. Liu, S. Xiang, X. Mo, S. Su, J. Zhang, Apoptosis and cytotoxicity of oligo (styrene-co-acrylonitrile)-modified montmorillonite, Appl. Clay Sci. 51 (2011) 214–219, https://doi.org/10.1016/j.clay.2010.11.019.
[55] R.L. Qi, R. Guo, M.W. Shen, X.Y. Cao, L.Q. Zhang, J.J. Xu, J.Y. Yu, X.Y. Shi, Electrospun poly(lactic-co-glycolic acid)/halloysite nanotube composite nanofibers for drug encapsulation and sustained release, J. Mater. Chem. 20 (2010) 10622, https://doi.org/10.1039/C0JM01328E.
[56] Z. Wang, Y.L. Zhao, Y. Luo, S.G. Wang, M.W. Shen, H. Tomas, M.F. Zhu, X.Y. Shi, Attapulgite-doped electrospun poly(lactic-co-glycolic acid) nanofibers enable enhanced osteogenic differentiation of human mesenchymal stem cells, RSC Adv. 5 (2015) 2383, https://doi.org/10.1039/C4RA09839K.
[57] S.G. Wang, R. Castro, X. An, C.L. Song, Y. Luo, M.W. Shen, H. Tomas, M.F. Zhu, X. Y. Shi, Electrospun laponite-doped poly(lactic-co-glycolic acid) nanofibers for osteogenic differentiation of human mesenchymal stem cells, J. Mater. Chem. 22 (2012) 23357, https://doi.org/10.1039/C2JM34249A.
[58] R.L. Qi, X.Y. Cao, M.W. Shen, R. Guo, J.Y. Yu, X.Y. Shi, Biocompatibility of Electrospun Halloysite Nanotube-Doped Poly(Lactic-co-Glycolic Acid) Composite Nanofibers, J. Biomater. Sci., Polym. Ed. 23 (2012) 299, https://doi.org/10.1163/092050610X550340.
[59] M. Shen, L. Li, Y. Sun, J. Xu, X. Guo, R.K. Prud'homme, Rheology and Adhesion of Poly(acrylic acid)/Laponite Nanocomposite Hydrogels as Biocompatible Adhesives, Langmuir 30 (2014) 1636–1642, https://doi.org/10.1021/la4045623.
[60] S.A. Kardos, L.G. Sultatos, Interactions of the Organophosphates Paraoxon and Methyl Paraoxon with Mouse Brain Acetylcholinesterase, Toxicol. Sci. 58 (2000) 118–126, https://doi.org/10.1093/toxsci/58.1.118.
[61] a) V.E. Sobolev, M.O. Sokolova, R.O. Jenkins, N.V. Goncharov, Nephrotoxic Effects of Paraoxon in Three Rat Models of Acute Intoxication, Int. J. Mol. Sci. 22 (2021) 13625, https://doi.org/10.3390/ijms222413625;
b) L.S. Deshpande, D.S. Carter, K.F. Phillips, R.E. Blair, R.J. DeLorenzo, Development of status epilepticus, sustained calcium elevations and neuronal injury in a rat survival model of lethal paraoxon intoxication, Neurotoxicology 44 (2014) 17–26, https://doi.org/10.1016/j.neuro.2014.04.006.
[62] N. Hrvat, Z. Kovarik, Counteracting poisoning with chemical warfare nerve agents. Counteracting poisoning with chemical warfare nerve agents, Arch. Ind. Hyg. Toxicol. 71 (2020) 266–284, https://doi.org/10.2478/aiht-2020-71-3459.
[63] M.A. Chagas, E.S. Pereira, J.C.S. Da Silva, W.R. Rocha, Theoretical investigation of the neutral hydrolysis of diethyl 4-nitrophenyl phosphate (paraoxon) in aqueous solution, J. Mol. Model. 24 (2018) 259, https://doi.org/10.1007/s00894-018-3798-1.
[64] V.A. Okello, I.O. K'Owino, K. Masika, V.O. Shikuku, Reduction and Degradation of Paraoxon in Water Using Zero-Valent Iron Nanoparticles, Sustainibility 14 (2022) 9451, https://doi.org/10.3390/su14159451.
[65] J.E. Kolakowski, J.J. DeFrank, S.P. Harvey, L.L. Szafraniec, W.T. Beaudry, K.H. Lai, J.R. Wild, Enzymatic Hydrolysis of the Chemical Warfare Agent VX and its Neurotoxic Analogues by Organophosphorus Hydrolase, Biocat. Biotransform. 15 (1997) 297–312, https://doi.org/10.3109/10242429709003196.
[66] C. Wilson, N.P. Cooper, Investigating the breakdown of the nerve agent simulant methyl paraoxon and chemical warfare agents GB and VX using nitrogen containing bases, Org. Biomol. Chem. 16 (2018) 9285–9291, https://doi.org/10.1039/C8OB02475H.
[67] W. Katyshkina, M. Kraft, Preparation of chlorides and esters of arylphosphates. Catalytic effects in the reaction of phenols with phosphorus oxychloride, Zh. Obshch. Khim. 26 (1956) 3060-3062, J. Gen. Chem. USSR (Engl. Transl.) 26 (1956) 3407–3410.
[68] D. Robati, Pseudo-second-order kinetic equations for modeling adsorption systems for removal of lead ions using multi-walled carbon nanotube, J. Nanostructure Chem. 3 (2013) 55, https://doi.org/10.1186/2193-8865-3-55.